https://doi.org/10.1007/s11440-022-01702-6

BENTONITE SWELLING INTO A VOID UNDER SUCTION OR WATER FLOW

María Victoria VILLAR*, Carlos GUTIÉRREZ-ÁLVAREZ, Gemma CAMPOS

CIEMAT, Avd. Complutense 40, 28040 Madrid, Spain

*corresponding author (mv.villar@ciemat.es) ORCID: 0000-0002-7282-5613

Abstract

In the context of the deep geological disposal of nuclear waste and to improve the understanding of the homogenisation process of bentonite barriers, in particular with regards to the filling of technological voids, tests were performed with compacted FEBEX bentonite samples hydrated under limited axial swelling conditions. The samples were saturated from the top surface using the vapour transfer technique (imposing suctions of 6 and 0.5 MPa), or with deionised water injected at a low flow rate either from the bottom surface or from the gap on top.

The final water content of the samples saturated via vapour transfer was related to the suction imposed during the tests according to the water retention curve. Thus, the final water content of the samples tested under suction 6 MPa was lower and not enough to allow sufficient bentonite swelling to close the gap. In contrast, the samples saturated under suction 0.5 MPa reached higher water contents and were able to fill the gap before the equilibrium water content had been reached. In the tests performed with liquid water supplied through the gap, the samples were able to swell easily into the open void and the gap closed earlier than when hydration took place from the opposite end. In all the tests the final water content of the bentonite was higher and the dry density lower towards

the hydration surface. These gradients were more remarkable and persistent as the initial strain was larger. No completely homogeneous density or water content distribution was observed in any of the tests. These changes were also reflected in the pore size distribution. The pores of size larger than the upper limit of mercury intrusion porosimetry (~550 µm) were also quantified, which allowed a better representation of the pore size distribution of the more swollen samples. Although the void ratio corresponding to pores smaller than 200 nm (e_m) was initially higher, over time the volume of macropores (e_M) increased more, giving place to an overall decrease of the e_m/e_M ratio, which tended to be constant along the samples in the longest tests. In the first stages of hydration the macropore void ratio and size considerably increased close to the gap in the tests with saturation from it.

Keywords: bentonite; self-sealing; swelling; porosity; technological void

1 Introduction

The capacity of bentonite to seal voids has been known for long and thus, compressed sodium bentonite has been proposed for example as a wellbore-sealing agent in the oil and gas industry, and the plug placement, hydration and integrity have been demonstrated in the field and laboratory environments (e.g. [1], [2], [3], [4]). This swelling and filling capacity was one of the reasons to propose bentonite as main material to construct engineered barriers in nuclear waste repositories, which is the framework of the research presented here.

The only currently recognised practicable solution for final disposal of highly active and long-lived radioactive wastes is emplacement in a Geological Disposal Facility with a combination of natural and engineered barriers. Openings created during the construction of the repository are potential preferential pathways for water, gas and radionuclides migration and for this reason deposition galleries or holes and access galleries and shafts should be backfilled and sealed. Even so it seems inevitable that some voids and small openings –frequently referred to as technological or construction voids or gaps– are created during construction. For example, the design of clay barriers has been mainly based on using blocks of compacted bentonite, and gaps between them and between bentonite blocks and the host rock or the waste containers will be initially unavoidable (e.g. [5]). A review carried out by Wang et al. [6] of national disposal concepts and large-scale tests performed to simulate the engineered barriers in a repository concluded that the volume of technological gaps with respect to the barrier volume could be between 6 and 14% with void sizes of

up to 2.5 cm. However, in the FEBEX large-scale in situ test the gap on top of the buffer had a height of 4-5 cm [7].

The evidence provided by some large-scale in situ tests indicates that these voids will quickly seal if water availability is enough [8], [7]. However, under limited water supply, as may be the case in some argillaceous host rocks, the closing of gaps may take much longer. In both cases the bentonite mass redistribution necessary to fill the void may lead to barrier inhomogeneities in terms of water content and dry density of the bentonite. These might have repercussions on the subsequent performance of the barrier, since the thermo-hydro-mechanical properties of the bentonite depend mainly on its dry density and water content. The heterogeneity of the barrier could also result in the development of preferential flow paths that can significantly affect gas transport, which would predominantly take place along areas of larger interconnected pores and hence, higher permeability [9], [10], [11]. Although the bentonite buffer shows a natural tendency towards homogenisation, long-term observations both in large-scale and in laboratory tests revealed that a degree of heterogeneity may persist in barrier materials even after full saturation (e.g. [8], [7], [12], [13]).

In this context, the overall objective of the BEACON (Bentonite Mechanical Evolution) project was to evaluate the consequences of heterogeneities on the performance of bentonite barriers in geological repositories for high-level radioactive waste. The objective of the investigation presented here, performed in the framework of BEACON, was to obtain qualitative and quantitative information about the evolution, at laboratory scale, of homogeneous bentonite samples (compacted blocks) upon hydration with the possibility of swelling into an axial void. Both in the laboratory and in the real case, this evolution might be affected by the characteristics of the barrier system (the particular dry density and water content of the barrier, the kind of bentonite) and by the boundary conditions, such as the size and location of the gaps, temperature and water salinity and availability. In this respect, the performance of simple well-designed small-scale laboratory tests addressing individual relevant phenomena is likely to be the most efficient way to advance knowledge [14]. Hence, in the present research a series of tests were performed to follow the density and water content changes in compacted bentonite samples saturated under limited axial swelling conditions and at the same time observe the closing of the initial gap. Two factors potentially affecting the closing of voids were analysed: water availability and gap location. Thus, the tests were performed either under constant water pressure conditions, simulating a repository excavated in crystalline host rock with plenty of water, or under controlled suction, simulating a repository with scarce water availability. An additional variable analysed in this work was the influence of hydrating through the gap or through

the part of the bentonite block opposite to the gap. FEBEX bentonite initially compacted with its hygroscopic water content (~14%) at a nominal dry density of 1.7 g/cm^3 was used in all the tests.

Wang et al. [6] performed a series of swelling tests with a sand/bentonite mixture compacted to different dry densities in an oedometer with a technological void of 14% on top and saturation through the bottom. They found a unique relation between dry density and axial pressure, irrespective of the samples having swollen into a void or not. The authors conclude that both macropores inside the material and technological voids played a similar role and became filled by particle exfoliation upon hydration. However, Bian et al. [15] reported an investigation in which compacted bentonite samples were saturated through technological voids on top. They observed that the swollen bentonite filled the initial voids first and then underwent compression by the swelling of the bentonite behind, which brought about significant changes in the bentonite microstructure.

Dueck et al. [16] summarised results of a series of tests in which the swelling of bentonite into axial and radial voids with free access to water was analysed. Two kinds of bentonite were used and under all testing conditions dry density gradients remained in the bentonite after full swelling and stress stabilisation were reached. Part of these tests were used in a modelling benchmark performed in the framework of BEACON, and it was concluded that the most difficult situation to model was the transient phase of the process of swelling into a gap [17]. More recently, and also inside the BEACON project, Harrington et al. [18] performed a series of tests to investigate the homogenisation and swelling capacity of a bentonite sample as it swelled into an engineering void as a function of the initial sample size, bentonite composition (calcic or sodic) and swelling orientation (axial or radial). The cells used allowed the measurement of flow rate as well as swelling pressure and pore pressure at different locations. They observed slow evolution in the rates of change in swelling and pore water pressure and, at the end of the tests, persistent differential stresses and non-uniform distribution of moisture contents, which was interpreted as an indication that full homogenisation might not eventually occur.

The set of tests included in this paper present the originality with respect to similar laboratory tests as those briefly described above, that hydration took place with liquid water or with water vapour, which may better reproduce the situation in some disposal concepts with limited water availability. In fact, this research showed that the way of hydration greatly affects the closing of gaps and the bentonite homogenisation process. The microstructural changes occurred in the bentonite during gap filling have been analysed by mercury intrusion porosimetry, assessing also the pores larger than

the equipment detection limit (550 µm) following the procedure recently devised by [19]. This kind of large pores was relevant in areas close to the gap in the first stages of hydration. Subsequently, the analysis of results has been performed focusing on the changes in the relation between the void ratios corresponding to the two major pore size families (macro and micropores, *sensu lato*), which is useful to validate double structure models.

2 Material

The FEBEX bentonite is a 900-t batch of bentonite extracted from the Cortijo de Archidona quarry (Almería, Spain) and processed in 1996 for the FEBEX project. The processing consisted of homogenisation, air-drying and manual removing of volcanic pebbles on-site and, at the factory, crumbling, drying in a rotary oven at clay temperatures between 50 and 60°C and sieving through a 5-mm mesh. The physico-chemical properties of the FEBEX bentonite, as well as its most relevant thermo-hydro-mechanical and geochemical characteristics obtained during the FEBEX project were summarised in e.g. [20] and updated in e.g. [21].

The smectite content of the FEBEX bentonite is close to 90 wt.%. The smectitic phases are actually made up of a montmorillonite-illite mixed layer, with 10-15 wt.% of illite layers. Besides, the bentonite contains variable quantities of quartz (2±1 wt.%), plagioclase (3±1 wt.%), K-felspar (traces), calcite (1 wt.%) and cristobalite–trydimite (2±1 wt.%). The cation exchange capacity is 98±2 meq/100 g, the main exchangeable cations being calcium (33±2 meq/100 g), magnesium (33±3 meq/100 g) and sodium (28±1 meq/100 g). The predominant soluble ions are chloride, sulphate, bicarbonate and sodium.

The liquid limit of the bentonite is 102±4 %, the plastic limit 53±3 %, the density of the solid particles 2.70±0.04 g/cm^3, and 67±3 % of particles are smaller than 2 µm (the whole granulometric curve can be found in Fig. SM1 in online Supplementary Material). The hygroscopic water content in equilibrium with the laboratory atmosphere (relative humidity 50±10 %, temperature 21±3 °C) is 13.7±1.3 %. The external specific surface area is 67 m^2/g and the total specific surface area is about 725±47 m^2/g.

The swelling pressure (P_s, MPa) of FEBEX samples flooded with deionised water up to saturation at room temperature and constant volume conditions can be related to dry density (ρ_d, g/cm^3) through the following equation (taken from [22]):

$$\ln P_s = 6.77\rho_d - 9.07 \quad [1]$$

149 The difference between experimental values and this fitting is, on average, 25 percent.

150 The hydraulic conductivity (k_w, m/s) of the bentonite at room temperature is also exponentially
151 related to its dry density, according to the following empirical expressions:

152 for dry densities of less than 1.47 g/cm^3:

$$\log k_w = -6.00\ \rho_d - 4.09 \quad [2]$$

153 for dry densities in excess of 1.47 g/cm^3:

$$\log k_w = -2.96\ \rho_d - 8.57 \quad [3]$$

154 The variation in the experimental values with respect to these fittings is smaller for low densities
155 than it is for higher values, with an average –in absolute values– of 30 percent [22].

156 Relationships between suction and water content obtained for different bentonite dry densities
157 under isochoric conditions can be found in [23], [24], [25]. For a sample compacted at dry density 1.6
158 g/cm^3 with hygroscopic water content the initial suction value would be ~120 MPa.

159 3 Methodology

160 The objective of the tests was to follow the density and water content changes in a block sample
161 hydrated under limited axial swelling conditions and at the same time observe the closing of the
162 initial void. The bentonite was compacted inside stainless steel rings and a void was left on top. In all
163 cases the granulated bentonite was initially compacted with its hygroscopic water content (~14%) at
164 a target dry density of 1.7 g/cm^3. The hydration of the samples took place with water in the vapour
165 phase through the sample surface closest to the gap (GAP-vapour tests), or with liquid water (GAP-
166 liquid), either through the sample surface away from the gap or from the gap surface. The thickness
167 of the gaps (0.5 or 0.9 cm) was chosen to allow proper measurement of changes over time. The tests
168 were dismantled after different periods of time and the final water content and dry density of the
169 bentonite at different levels of the block sample were measured, as well as the pore size distribution.

3.1 GAP-vapour tests

In the GAP-vapour tests the samples were compacted in a cell with perforated lids, and saturated from the top surface, where the void was, using the vapour transfer technique (Figure 1), which consists in subjecting the sample to a certain relative humidity in a close container (vacuum desiccator). The diameter of the samples was 3.8 cm and the initial height was 2.49±0.02 cm, with a dry density of 1.71±0.01 g/cm^3. The bottom part of the cell was sealed, and on the top surface of the sample a porous ceramic filter was placed, so that water transfer took place through this porous medium. The initial gap thickness was of 0.47±0.03 cm. The evolution over time of the void closing and the changes in bentonite overall water content and dry density were followed by periodically measuring the gap height and weighing the cylinder with the sample inside (Fig. SM2). A total of 26 samples were tested and dismantled after different periods of time between 15 days and 15.5 months. The samples were subjected to relative humidities of 95.5 and 99.6% corresponding to total suctions of 6 and ~0.5 MPa, respectively, keeping a constant temperature of 20°C. These suctions were obtained by placing in the desiccators a sulphuric acid solution of concentration 10% and a sodium chloride solution of concentration 0.6%, respectively. It was checked that the concentration of the solutions barely changed during the stabilisation process, because the volume of solution used was high with respect to the volume of water adsorbed by the samples.

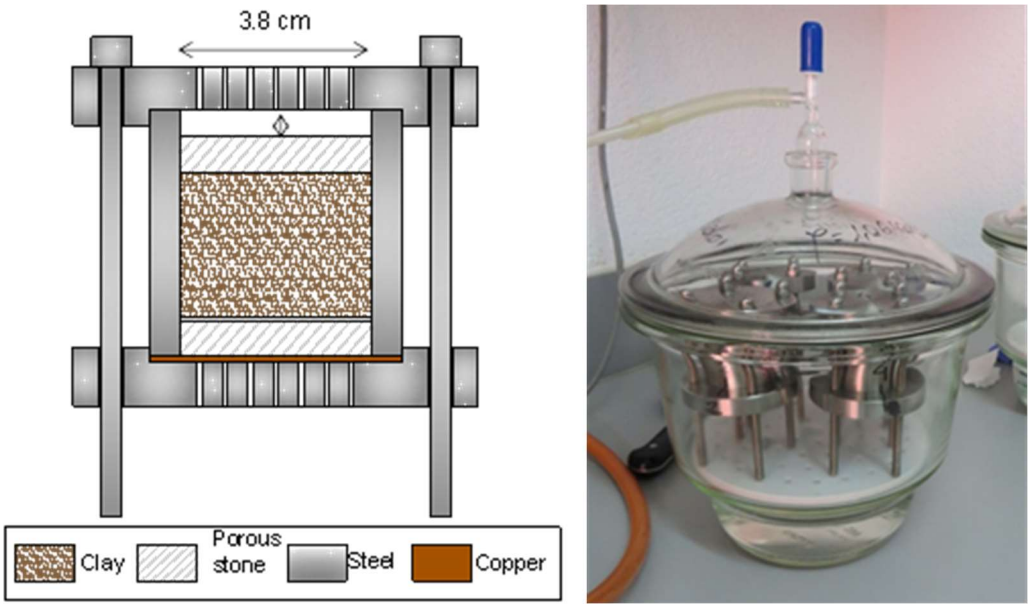

Figure 1. Schematic representation of the GAP-vapour test cells and desiccator with cells inside

3.2 GAP-liquid tests

The initial characteristics of the samples were the same for all the tests: the bentonite was compacted with its hygroscopic water content (14.0±0.5) inside the cell ring applying a uniaxial pressure of ~30 MPa, giving place to an initial dry density of 1.67±0.02 g/cm^3. The diameter of the resulting samples was 5.0 cm and the initial height 2.54±0.02 cm, leaving a gap of 0.88±0.02 cm on top of them. Note that the difference in gap height with respect to the GAP-vapour tests (0.9 vs 0.5 cm) allowed larger maximum swelling. The sample was sandwiched between porous ceramic filters which allowed a better distribution of water over the sample surface and offered a plane and homogeneous surface to limit swelling.

Deionised water was injected with a pressure/volume controller at a rate of 0.072 cm^3/h, the minimum allowed by the equipment, so that to avoid interference with the sample swelling and to make the process as slow as possible. Six tests in which the bentonite block was hydrated from the surface opposite to the gap and six with hydration from the gap were performed and dismantled after different hydration times (see Table 1 and Table 2 for details of each test). The part of the cell opposite to the hydration surface was open to atmosphere. Figure 2 shows the configuration for the tests with water injection opposite to the gap. In the set of tests with saturation through the gap (except in the first one, GL6), the porous filter was saturated outside the cell prior to the start of the tests. Injection pressure was atmospheric at the beginning of the tests, since the flow rate was prescribed. Both injection pressure and water intake were measured online.

The tests were performed at laboratory temperature.

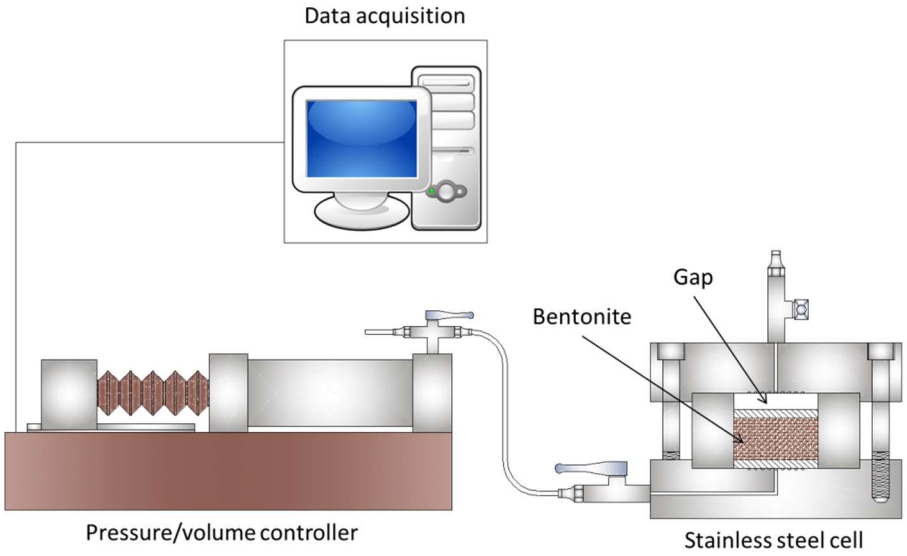

Figure 2. Schematic representation of the assembly for GAP-liquid tests (injection opposite to gap)

3.3 Postmortem tests

At the end of the two kinds of tests the samples were measured, weighed, and cut in transversal sections (Fig. SM3). In each section subsamples were obtained to determine water content, dry density and pore size distribution. Three sections were usually defined, because a minimum section volume was necessary to obtain subsamples coherent enough to determine their dry density.

Dry density (ρ_d) is defined as the ratio between the mass of the dry sample and the volume occupied by it prior to drying. The volume of the specimens after extraction from the cell was determined by measuring their dimensions, whereas the volume of the subsamples of each section was determined by immersing them in a recipient containing mercury and by weighing the mercury displaced, considering a density of mercury of 13.6 g/cm^3. The precision of this measurement is between 0.01 and 0.02 g/cm^3. The mass of water was determined as the difference between the mass of the sample and its mass after oven drying at 110°C for 48 hours. The gravimetric water content (w) is defined as the ratio between the mass of water and the mass of dry solid expressed as a percentage. The precision of this measurement is about 0.2%. The water content was usually determined in the subsamples used for the dry density determination and also in an additional subsample of each section.

The pore size distribution of the subsamples was determined by mercury intrusion porosimetry (MIP). The mass of the subsamples used was between 2.54 and 0.54 g. The samples were put in the

ice condenser of a Telstar LioQuest equipment at -30°C for 3 hours. Subsequently, they were lyophilised for 22 hours at a temperature of -50°C under a vacuum of 0.2 mbar, so that to eliminate the water in the pores by sublimation. Thereafter, they were heated at 25-30°C for 3 hours. The samples were later kept in a desiccator until the MIP analysis. The porosimeter used was a Micromeritics AutoPore Series IV 9500, which allowed the exploration of pore diameters between approximately 0.006 and 600 µm. Prior to mercury injection the sample was outgassed by applying a vacuum of 50 µm-Hg. Afterwards the mercury injection pressure was increased from 2.7 kPa to 220 MPa in 109 steps. To determine the extrusion branch of the curve, the pressure was released in 56 steps down to a pressure of 68.6 kPa. A contact angle of mercury of 139° both on advancing and of receding on the clay surface was considered (for information about mercury contact angle on clays see for example [26], [27]).

4 Results

4.1 GAP-vapour tests

4.1.1 Evolution over time

The lids of the GAP-vapour cells were unscrewed every week and the cell with the sample inside was weighed and the height of the gap measured (Figure SM1). Thus the evolution over time of the overall bentonite water content and dry density was approximately followed. Since the bentonite was compacted with hygroscopic water content, the initial suction of the samples was very high, about 100 MPa. For this reason all the samples took water under the two suctions applied (6 and 0.5 MPa), swelled and tended to close the gap. The final values of dry density and water content for each test performed under suctions 6 and 0.5 MPa are plotted in Figure 3. Since the tests had different durations this Figure also gives a temporal evolution (the evolution of the overall water content and dry density in each of the tests performed are shown in Fig. SM4 and SM5). All the tests were performed in duplicate.

In the first stages, for times shorter than 40 days, the samples under 6 MPa took more water and swelled more. For longer equilibration times the trend inverted and consequently the final water contents of samples under 0.5 MPa were higher and their dry densities lower. After approximately 100 days the equilibrium water content for a suction of 6 MPa was reached (~25%). The gap was not completely closed in the tests performed under 6 MPa, which indicates that the swelling capacity of the bentonite under this suction was lower than 20%. In the tests performed under 0.5 MPa, the gap

was closed at a time between 100 and 180 days (at that time the dry density had reached its lower possible value). Also, for suction 0.5 MPa the water content remained constant (~33%) after less than 200 days, which is probably related to the fact that no further swelling was allowed.

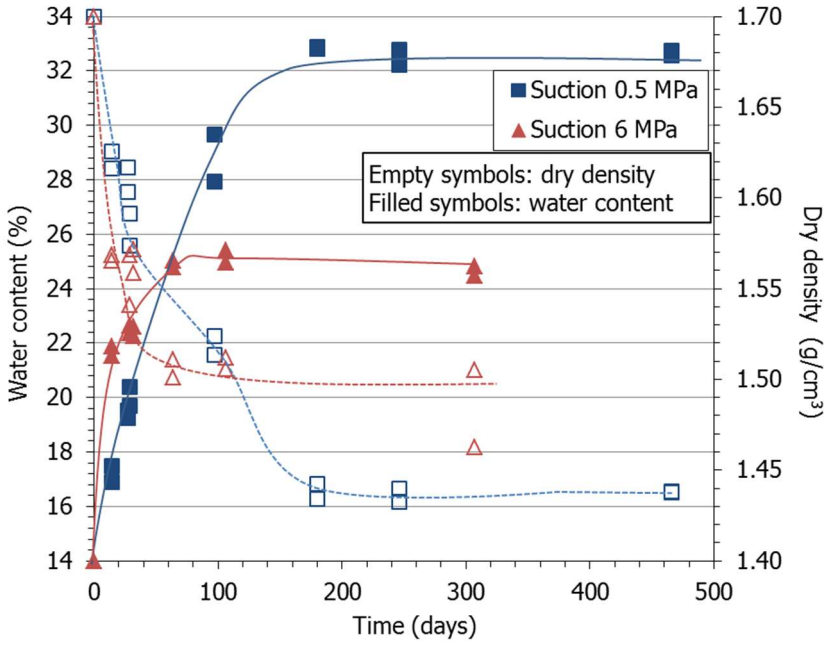

Figure 3. Final values of overall dry density and water content in the GAP-vapour tests (the curves just indicate approximate trends)

4.1.2 Final physical state

After different equilibration times the cells were dismantled, the bentonite weighed and measured and cut into sections for the postmortem determinations, as described in 3.3. The results obtained for the different subsamples in terms of water content and dry density are plotted in Figure 4. The shorter tests showed a water content gradient from top to bottom. Towards the top of the sample, where the void was, the water content was higher and the dry density lower. In fact, the upper surface of the sample was usually uneven and crumbled easily, since it swelled into a void under free swelling conditions (Figure 5). For this reason it was difficult in some cases to cut the upper subsamples and determine their dry density, which was lower. The dry density gradients kept even in the longer tests, although in the samples tested under suction 0.5 MPa were less steep and kept more or less constant as the overall water content increased and the overall dry density decreased. This could be related to the slower hydration under the lowest suction (Figure 3).

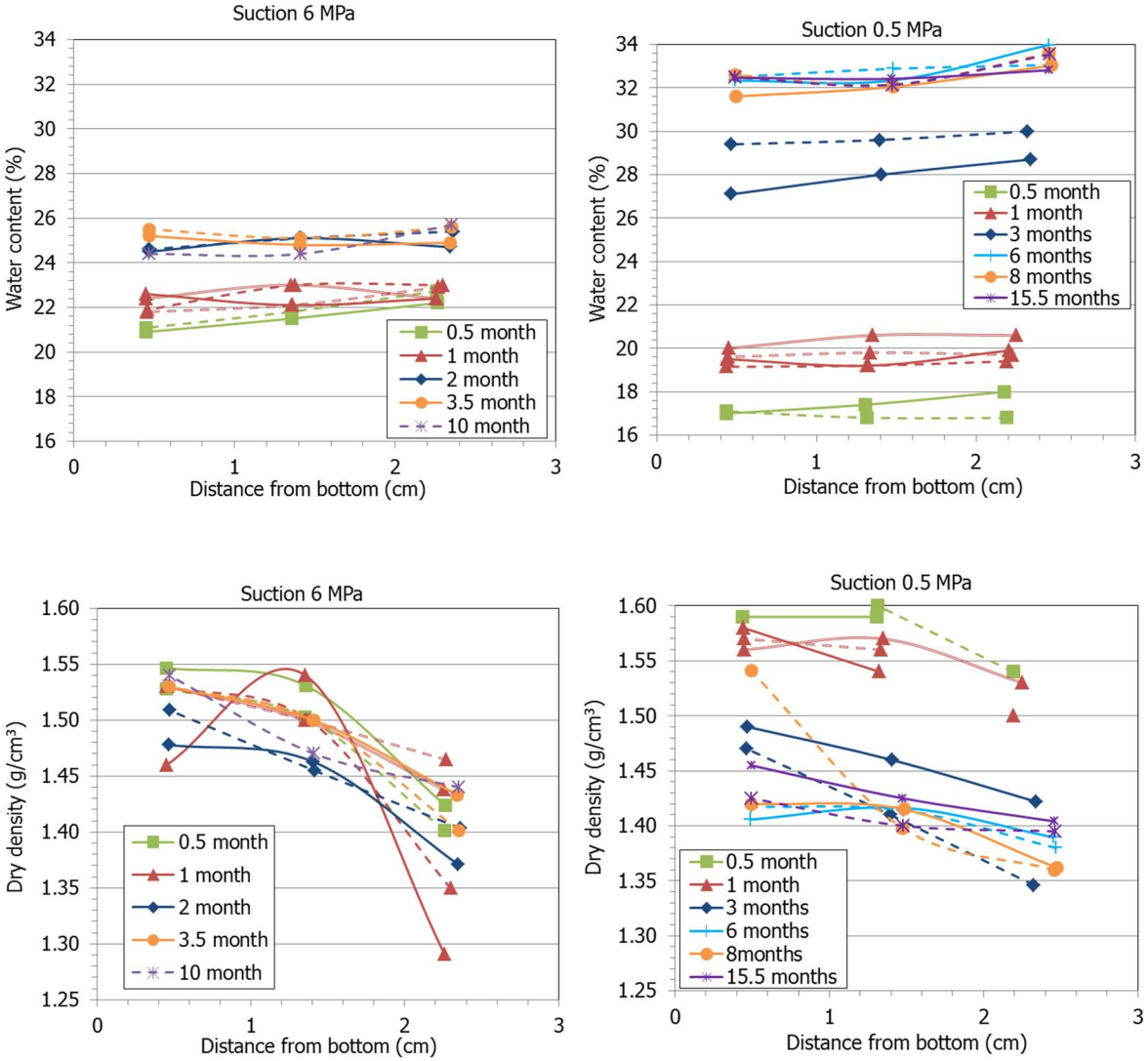

278

279

280 **Figure 4. Final water content of subsamples of the tests performed under suction 6 MPa (left) and 0.5 MPa (right)**

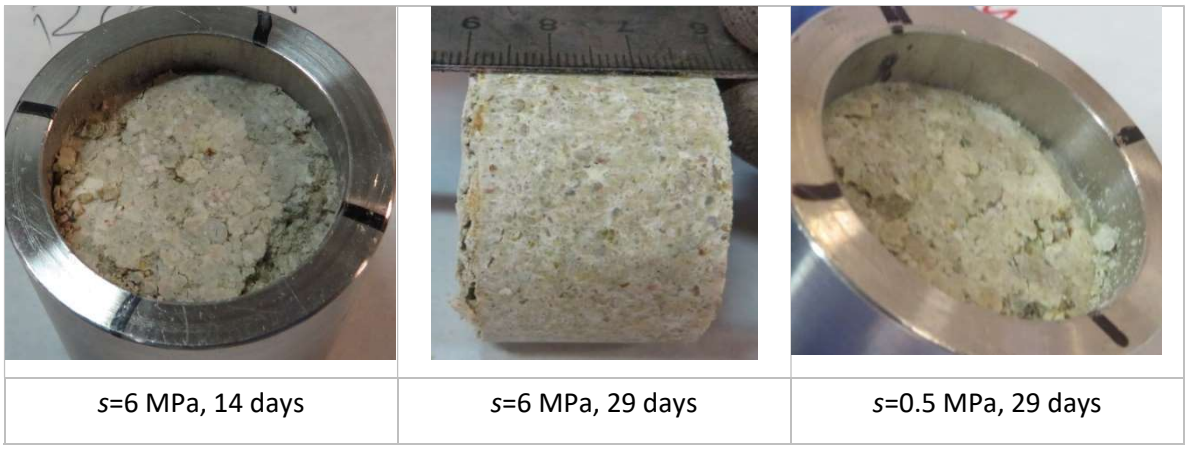

s=6 MPa, 14 days	*s*=6 MPa, 29 days	*s*=0.5 MPa, 29 days

281 **Figure 5. Appearance upon dismantling of some of the shorter GAP-vapour tests**

4.1.3 Pore size distribution

From each cell three subsamples taken at different distances from the gap were used to determine the pore size distribution by MIP. The determination was performed in subsamples of all the cells, but only those corresponding to the shorter and longer tests performed under suction 0.5 MPa are shown in Figure 6, which includes the incremental curves of mercury intrusion as a function of the mean pore diameter of the diameter size intervals corresponding to each pressure increase step. The curve for a FEBEX sample compacted with approximately the same dry density and water content as the initial conditions used in the cells (1.69 g/cm^3, 13.5%) is also included (labelled "Initial"). For all the samples there were two pore families corresponding to pores larger and smaller than approximately 200 nm with diameter modes of 19 µm and 11 nm, respectively. In several thermo-hydro-mechanical models (e.g. [28]), this pore size represents the limit separating inter-aggregate from intra-aggregate pores, the latter not affected by density changes. There is discussion on the criteria that can be followed to select this delimiting value [29]. The 'valley' criterion was chosen in this work, consisting of using the lowest point of the valley between the two peaks of a bimodal distribution. According to the usual pore size classification [30], the first family identified would be in the range size of the macropores (larger than 50 nm) and the second one in that of the mesopores (between 50 and 2 nm). The Figures show that the volume of pores larger than 200 nm increased during testing, particularly as the test was longer. The mode size of the macropores also tended to increase, from an initial diameter mode of 19 µm to values of up to 80 µm in the tests under suction 0.5 MPa and up to 100 µm in the tests under suction 6 MPa, in both cases with a few subsamples of the shorter tests showing much higher sizes. The mode of the mesopores did not change much with respect to the original value, remaining in sizes of 12±4 nm with no particular trends.

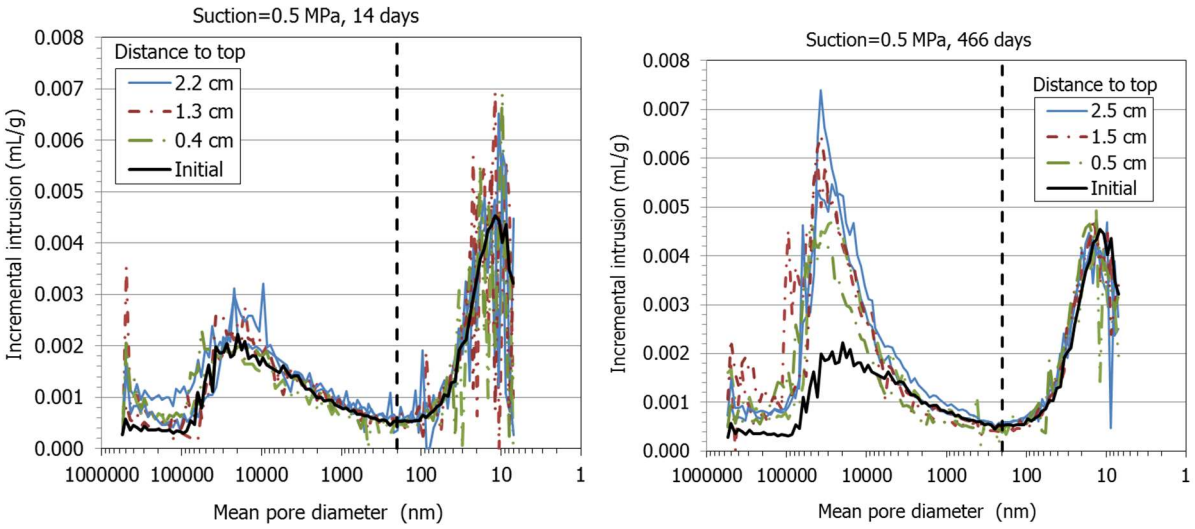

304

305 **Figure 6. Pore size distribution of subsamples tested in GAP-vapour cells under suction 0.5 MPa for two different times**
306 **and for the initial block expressed as incremental mercury intrusion (duplicate samples for each duration)**

307 The mercury intrusion method allows access to be gained only to part of the macroporosity (pores of
308 diameter smaller than ~550 µm) and to part of the mesopores (those of diameters larger than 7 nm),
309 since mercury does not intrude the microporosity (pores of a size of less than 2 nm). An estimation of
310 the percentage of pores actually intruded can be made by comparing the actual void ratio of the
311 samples (computed from their dry density and density of solid particles) and the apparent void ratio
312 calculated from mercury intrusion by the equipment software. Thus, the percentage of pores
313 intruded by mercury in these subsamples was between 42 and 74%. The non-intruded porosity is
314 usually associated in compacted clays to the pores of a size smaller than the limit of the apparatus
315 (~7 nm). There is uncertainty in this approach, since it is possible that pores larger than 7 nm were
316 not intruded because of the bottleneck effect. All of the volume of such pores will be allocated to the
317 threshold radius class of the most restricted part of the entryway, which will result in an
318 overestimation of the smaller pore sizes volume. Likewise, although in compacted clay materials
319 pores larger than those that can be quantified by MIP are not expected, pores of this size (i.e. >550
320 µm) could be present in the samples closest to the gap of the shorter tests, which were friable and
321 crumbly. A visual inspection of the samples upon dismantling allowed to conclude that this was the
322 case for the upper part of the samples shown in Figure 5, all of them corresponding to tests shorter
323 than 32 days.

324 Hence, to take into account the large pores observed in those upper subsamples, an estimation of
325 the volume of pores larger than 550 µm was made following this approach [19]:

At the beginning of a MIP test the calibrated sample holder is filled with mercury under a low injection pressure. Considering the sample mass and the volumes of the sample holder and of the mercury intruded, the dry density of the sample is computed by the equipment software. This initial mercury injection is considered by the equipment as the zero value for the rest of the MIP test, which actually starts when injection pressure is increased above this value. Thus, all the large porosity filled during this initial step is disregarded. The comparison between the dry density determined by the equipment at this step and the actual dry density of the sample allows estimating the volume of pores larger than 550 μm: when the sample contains a significant volume of large pores, the dry density determined by the porosimeter is considerably higher than the actual dry density of the sample, whereas if there are not large pores the two values tend to be similar.

Taking all the above into account, the void ratio corresponding to pores larger and smaller than 200 nm (e_M and e_m, macro and micro, respectively) was recalculated, assuming that the non-intruded porosity corresponded to pores smaller than the equipment injection capacity and, in some upper subsamples, also to pores larger than 550 μm. The evolution of void ratio over time corresponding to pores larger and smaller than 200 nm is plotted in Figure 7 as a function of the position along the sample for the two suction values. In all cases the largest proportion of void ratio corresponded to the pores of diameter smaller than 200 nm, the volume of which increased during testing with respect to the reference sample. Also, the percentage of void ratio corresponding to pores larger than 200 nm increased with respect to the reference sample, since the total void ratio increased because of the bentonite swelling into the gap and overall dry density decrease. In fact, the highest increase in void ratio was experienced by the samples closest to the gap, which agrees with their lower dry density (Figure 4). The overall void ratio increase took place very quickly in the samples tested under 6 MPa (it was already clear after 15 days) but took longer in the samples tested under suction 0.5 MPa. This agrees with the different hydration kinetics of the two sets of tests commented above (Figure 3) and would indicate that hydration under free swelling conditions brought about an increase in the volume of all pore sizes. Furthermore, in all the tests performed under suction 6 MPa the macropore void ratio was higher in the subsample closest to the gap than in the other subsamples. In contrast, this difference among subsamples was less clear in the longer tests performed under suction 0.5 MPa.

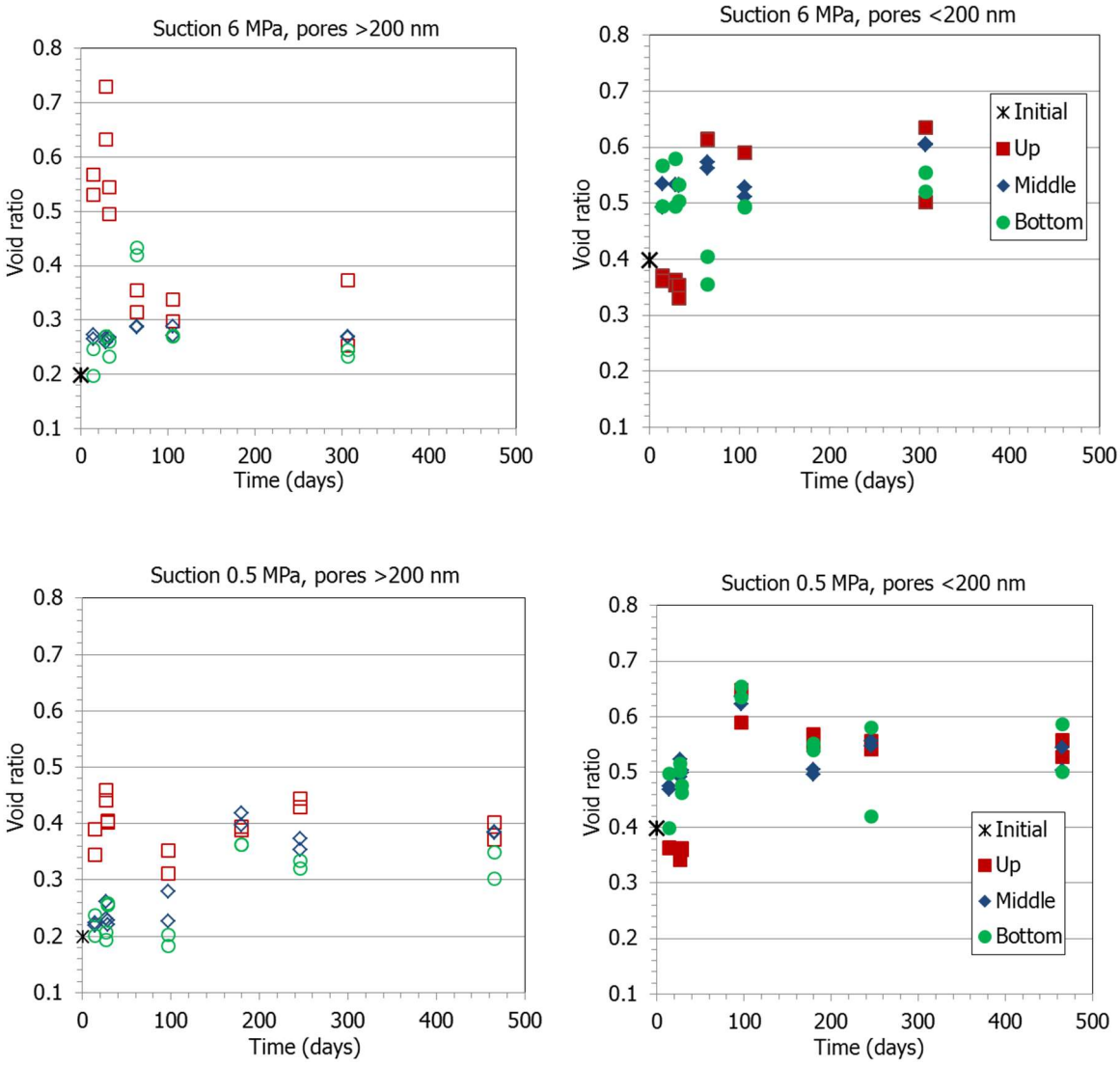

Figure 7. Evolution of void ratio over time corresponding to pores larger and smaller than 200 nm for subsamples of the two sets of GAP-vapour tests taken at different heights along the bentonite blocks. The crosses indicate the values for the initial sample (time 0)

In the tests under suction 0.5 MPa, close to the gap the macropore void ratio quickly increased, but then remained almost constant. In the middle part of the sample the increase in macropore void ratio was more gradual and reached a maximum after 180 days (when the gap was already closed), remaining constant afterwards. For the bottom part of the sample the increase in macropore void ratio took place only after 100 days. The increase in micropore void ratio was more uniform across a given sample, had a maximum after 97 days (once the gap was closed) and then remained approximately constant. In the tests under suction 6 MPa, there was a quick and huge increase in macropore void ratio close to the gap that was reduced after two months and then did not change much. In this respect, Figure 8 shows the appearance of the upper part of a sample saturated under

suction 6 MPa after 14 days and just before dismantling it after more than 300 days. It is clear that the initial disruption of the sample, likely with creation of macropores, was healed over time, even though the gap was not closed. The changes in the size of the macropores over time ran in parallel with those of the macropore void ratio. The middle and bottom parts of the samples behaved similarly over time, with the pores smaller than 200 nm accounting for most of the overall increase in void ratio.

s=6 MPa, 14 days	*s*=6 MPa, 307 days

Figure 8. Appearance of a GAP-vapour sample saturated under suction 6 MPa at an intermediate stage (14 days, left) and just before dismantling it (right)

As a consequence of these changes in the pore size distribution, the ratio between the void ratio corresponding to pores smaller (e_m) and larger (e_M) than 200 nm was lower in the subsample closest to the gap for the tests shorter than 2 months performed under suction 6 MPa, whereas it remained similar to the initial one in the rest of subsamples (Fig. SM6). In the shorter tests (≤3 months) performed under suction 0.5 MPa, this ratio increased at the bottom and tended to decrease towards the part of the samples closest to the hydration surface (gap), which resulted from the increase in the percentage of macropores in the most hydrated bentonite. Over time these differences inside a given sample were obliterated by the increase in void ratio corresponding to larger pores. As a result, all the subsamples from larger tests (≥6 months), those in which the gap was closed, had e_m/e_M ratios lower than the initial one and similar among them, which would be an additional indication of equilibrium being reached.

4.2 GAP-liquid tests

The tests in which the bentonite was saturated with liquid water were performed either injecting the water from the surface of the block opposite to the gap, or from the gap surface. The initial characteristics of the samples were the same in both cases for all the tests: hygroscopic water content, nominal dry density of 1.7 g/cm^3, nominal height of 2.5 cm, a gap of 9 mm on top of them (Figure 2). For the GAP-liquid tests only the state of the sample at the end of each test is available, because their state could not be periodically checked without disturbing too much the state of the samples.

4.2.1 Evolution over time

Six tests in which the bentonite block was hydrated from the surface opposite to the gap and six with hydration from the gap were performed and dismantled after different hydration times (Table 1 and Table 2). At the beginning of the tests, a low flow rate was prescribed (0.07 cm^3/h) and the injection pressure was atmospheric. In order to keep the flow rate prescribed, the injection pressure started to increase after ~7 days from the beginning of water injection in the tests with hydration through the bottom and after 11 days in the other tests (Fig. SM7). The overall degree of saturation of the samples when the injection pressure started to increase was between 57 and 74% in the samples saturated from the bottom and between 75 and 87% for the others. In all cases the outlet of the cell opposite to hydration remained open to atmosphere during the whole duration of the test, except in the case of the longest test of each kind (GL1 and GL13), in which the outlet had to be closed towards the end of the tests to avoid water going out.

During the first test with hydration from the top void, GL6, it was realised that it was no possible to identify how much water had been actually taken by the porous filter on top, by the bentonite, or had gone between the porous filter and the cell wall. To partly solve this uncertainty, in the rest of the tests the upper porous filter was saturated outside the cell prior to test initiation.

Table 1. Initial and final characteristics of the GAP-liquid tests with hydration through the bottom

Test	Duration (days)	Initial w (%)	Initial ρ_d (g/cm^3)	Initial S_r (%)	Initial sample h (cm)	Initial gap h (cm)	Final w (%)	Final ρ_d (g/cm^3)	Final S_r (%)	Final sample h (cm)	Final gap h (cm)
GL1	63	13.3	1.65	57	2.58	0.83	45.2	1.25	103	3.41	0.00
GL2	14	13.3	1.67	59	2.54	0.87	32.2	1.32	83	3.21	0.20
GL3	28	13.8	1.67	60	2.53	0.90	44.9	1.23	102	3.43	0.00

Test	Duration (days)	Initial w (%)	Initial ρ_d (g/cm^3)	Initial S_r (%)	Initial sample h (cm)	Initial gap h (cm)	Final w (%)	Final ρ_d (g/cm^3)	Final S_r (%)	Final sample h (cm)	Final gap h (cm)
GL4	7	14.3	1.67	62	2.52	0.89	24.1	1.50	81	2.81	0.60
GL5	4	14.4	1.66	62	2.55	0.85	18.9	1.58	72	2.69	0.70
GL12	10	13.1	1.69	59	2.52	0.90	26.3	1.43	80	2.98	0.44

414

415 **Table 2. Initial and final characteristics of the GAP-liquid tests with hydration from gap**

Test	Duration (days)	Initial w (%)	Initial ρ_d (g/cm^3)	Initial S_r (%)	Initial sample h (cm)	Initial gap h (cm)	Final w (%)	Final ρ_d (g/cm^3)	Final S_r (%)	Final sample h (cm)	Final gap h (cm)
GL6	7	14.3	1.66	62	2.55	0.87	29.0	1.22	64	3.42	0.00
GL7[a]	7	14.4	1.67	63	2.54	0.88	33.6	1.22	75	3.42	0.00
GL8[a]	22	14.1	1.67	61	2.56	0.85	45.1	1.25	105	3.41	0.00
GL9[a]	14	13.6	1.70	63	2.53	0.89	41.2	1.26	98	3.41	0.00
GL11[a]	2	14.3	1.67	62	2.51	0.91	18.3	1.47	59	2.87	0.78
GL13[a]	39	14.3	1.66	63	2.55	0.87	45.8	1.24	104	3.42	0.00

416 [a] upper porous filter saturated before starting water injection

417

418 The overall water content and dry density of the samples at the end of the tests are plotted in Figure
419 9. Although the flow rate was the same in all the tests, the Figure seems to indicate that for a given
420 hydration time the water content was lower in the tests hydrated opposite to the gap. This is
421 because in these tests the porous stone had to be saturated before water reached the bentonite,
422 whereas in the other test series, since the porous stone was saturated before assembling the cell, the
423 bentonite started to take water at the beginning of the test, when the bottom inlet was open (Figure
424 2). The dry density decreased initially faster and reached earlier the lowest possible value when the
425 bentonite was hydrated from the gap. As a result, the gap closed sooner when hydration occurred
426 from the gap surface (Table 1, Table 2 and Fig. SM8). It took 7 days for the gap to close in this case
427 and about 30 days when hydration took place from the opposite surface. However, the injection
428 pressure started to increase later in the tests saturated through the gap (Fig. SM7), which might be
429 related to the lower density (see next section), and hence higher permeability, of the area close to
430 the gap. In the tests with saturation opposite to the gap, the injection pressure started to increase

before the gap was completely closed, and this could have had some influence on the swelling deformation evolution. The samples were already fully saturated when the gap closed up. However this was not the case in the tests saturated through the gap, which was closed before the samples were completely saturated (Table 2).

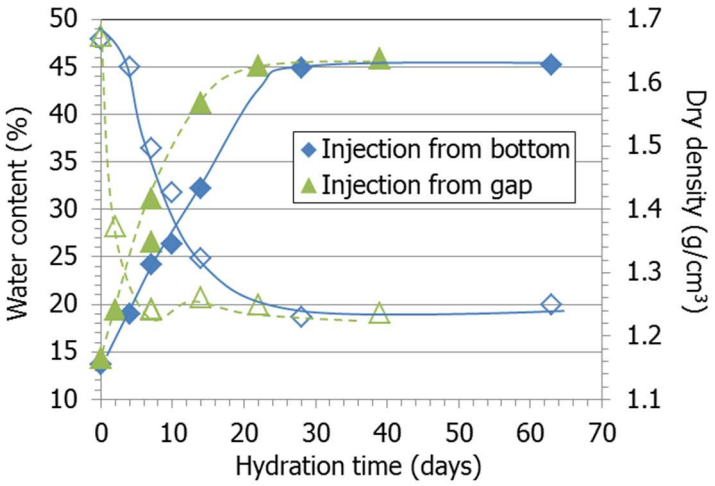

Figure 9. Evolution of water content (filled symbols) and dry density (empty symbols) in GAP-liquid tests (the curved lines indicate approximate trends). In the tests with hydration from the gap the porous stone was saturated prior to cell assemblage

4.2.2 Final physical state

Figure 10 shows a comparison of the final water content and dry density distribution along the height of the samples from all the tests. The values are plotted as a function of the distance from the hydration surface, which was the bottom of the cell in the tests with saturation opposite to the gap, and the top of the cell in the cells with saturation through the gap (in both cases considering also the thickness of the porous filter).

The overall water content increased with time but was always higher towards the hydration surface. In the same way the dry density decreased as the gap was filled and was always lower towards the hydration surface. Although the gradients attenuated in the long term, they did not disappear, not even when the sample was completely saturated: the water content near the hydration surface remained higher and the dry density lower (tests GL1, GL3, GL8 and GL13). Out of these longer tests, those saturated through the gap showed slightly steeper gradients. In the tests saturated from the bottom the water content and dry density along the sample seems to have reached a steady state after ~28 days (compare results of GL3 and GL1). In contrast, in the tests saturated from the gap, although after 22 days (test GL8) the sample was virtually saturated, the water content and dry

density distributions along the sample differed with respect to those after 39 days (test GL13): the water content close to the gap had reached its higher value, but had not equilibrated yet farther away from the gap. As well, the dry density close to the gap increased from 22 to 39 days of hydration, while the contrary happened in the opposite end.

For a given test duration the water content was higher and the dry density lower in the samples hydrated through the gap, which agrees with the faster closing of the void, since the gap allowed for a quick swelling of the bentonite close to it. However, the difference in water content between the two test series is unexpected, since the same flow rate was used in both cases. The explanation may be that part of the water initially injected in the tests saturated through the bottom remained in the porous stone, which was initially unsaturated. Hence, the actual water inflow into the bentonite would be higher in the case of the tests hydrated from the gap, where the porous stone had been previously saturated. This would have made the bentonite saturation process (water intake) quicker in the latter case. As well, the water content and the dry density gradients for tests of similar duration tended to be higher in the samples saturated through the gap, which may be a consequence of the irreversible initial deformation of the bentonite close to the gap.

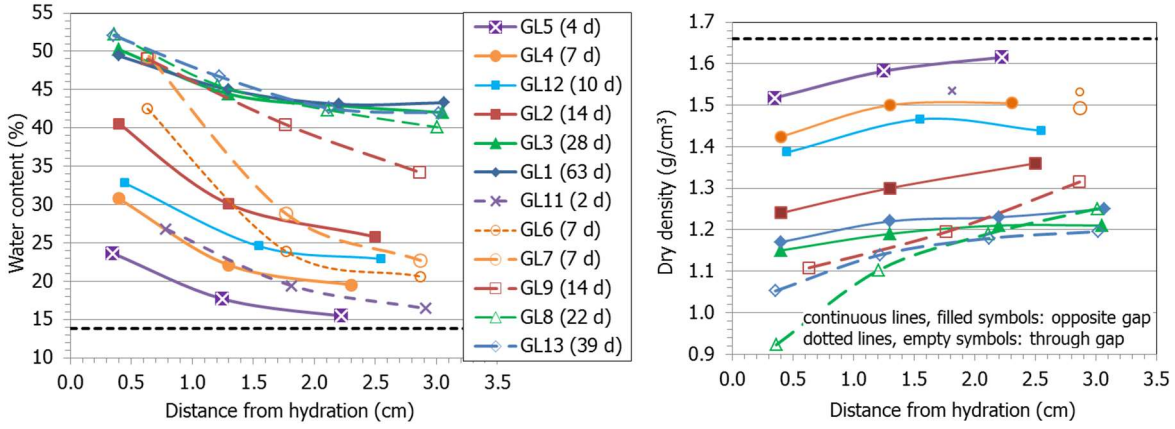

Figure 10. Final water content and dry density along the samples used for GAP-liquid tests. The thick discontinuous horizontal lines indicate the values for the initial sample. Series with filled symbols and continuous lines correspond to tests with hydration opposite to gap, and series with empty symbols and dotted lines correspond to tests with hydration from gap

4.2.3 Pore size distribution

The same analysis of the final pore size distribution described for the GAP-vapour tests was performed with the subsamples of the GAP-liquid tests. As an example for the tests saturated from the bottom, Figure 11 shows the incremental curves of mercury intrusion for the subsamples of the

tests lasting 14 and 63 days and for a FEBEX sample compacted with approximately the same dry density and water content as the initial conditions used in the cells (1.69 g/cm^3, 13.5%). In some tests it was not possible to get material from the upper part of the specimens (the one swelling into the void) for the MIP analysis because of its inconsistency. In fact, in the tests saturated from the gap the pore size distribution was only obtained for subsamples of tests GL9, GL11 and GL13 for lack of enough material. Again, two pore families corresponding approximately to pores larger and smaller than 200 nm could be told apart. The volume of pores larger than 200 nm increased during testing, particularly closer to the gap and as the test was longer. As well, the size of the macropores increased all along the samples and for all testing times, whereas the size of the mesopores remained in the range between 5 and 20 nm.

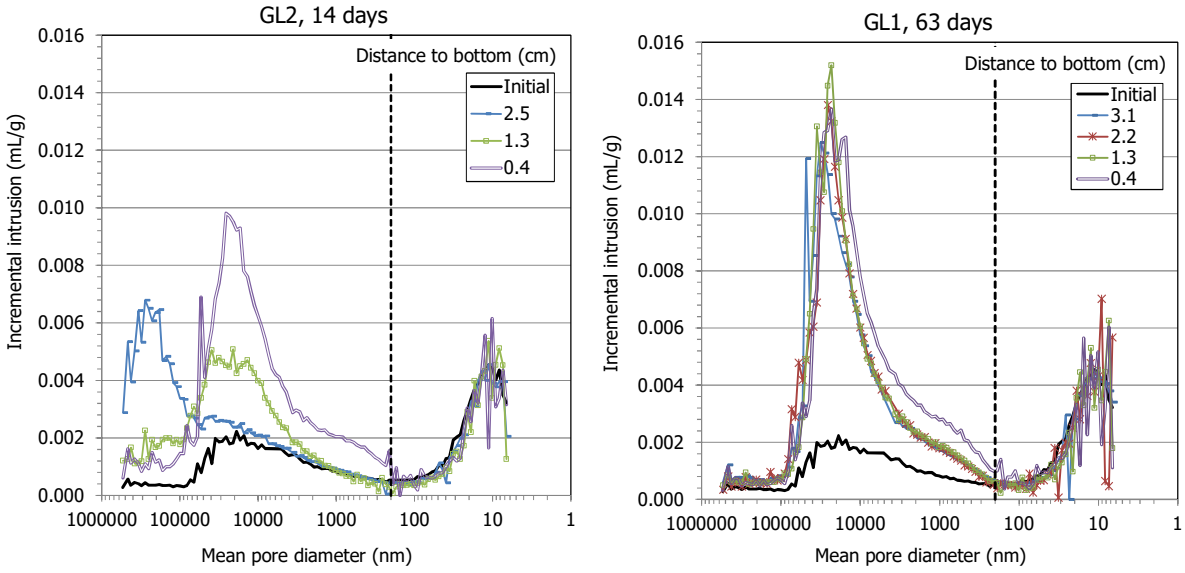

Figure 11. Pore size distribution of samples tested in GAP-liquid cells for 14 days (GL2) and 63 days (GL1) and for the initial block expressed as incremental mercury intrusion (water injection from bottom, opposite to gap)

The percentage of pores intruded by mercury in these subsamples was between 28 and 85%. As it was explained for the GAP-vapour tests, in some subsamples (those closest to the gap), part of the porosity not explored by the porosimeter may correspond to pores larger than 550 µm. This would be the case of the upper subsamples of the tests shorter than 14 days in the samples saturated from the bottom and shorter than 7 days in the samples saturated from the gap (the appearance of some of these samples is shown in Fig. SM9). Taking this into account, the void ratio corresponding to pores larger and smaller than 200 nm was calculated and is plotted in Figure 12 as a function of the hydration time and of the position of the subsample. Although the volume of pores smaller than 200

499 nm was initially higher, over time the volume of macropores increased more, and in fact the highest
500 void ratio in the bentonite from longer tests corresponded to macropores, irrespective of the way of
501 hydration. The initial changes were quicker and more drastic when hydration took place through the
502 gap: after only 2 days the subsample closest to the hydration surface (i.e. to the gap) experienced a
503 huge increase in the size of the macropores, which after 14 days considerably increased also in the
504 rest of subsamples, but more as the subsample was closer to the gap. The samples saturated through
505 the bottom experienced soon an increase in macropore void ratio at all locations. The micropore void
506 ratio also increased in the samples closest to hydration (i.e. the bottom) in the first stages of
507 hydration, but decreased with respect to the initial one close to the gap. Eventually, the micropore
508 void ratio also increased away from the hydration surface and a “steady microstructural state” was
509 reached after 30 days. Maybe the main difference between the samples saturated through the gap
510 or opposite to it in terms of microstructural evolution was that in the first case the increase of
511 macropore void ratio in the top and middle parts of the samples was quick and huge. Also, in these
512 samples the void ratio increase affected all pore sizes, whereas in the samples saturated opposite to
513 the gap the macropore void ratio increased gradually and more than that corresponding to smaller
514 pores.

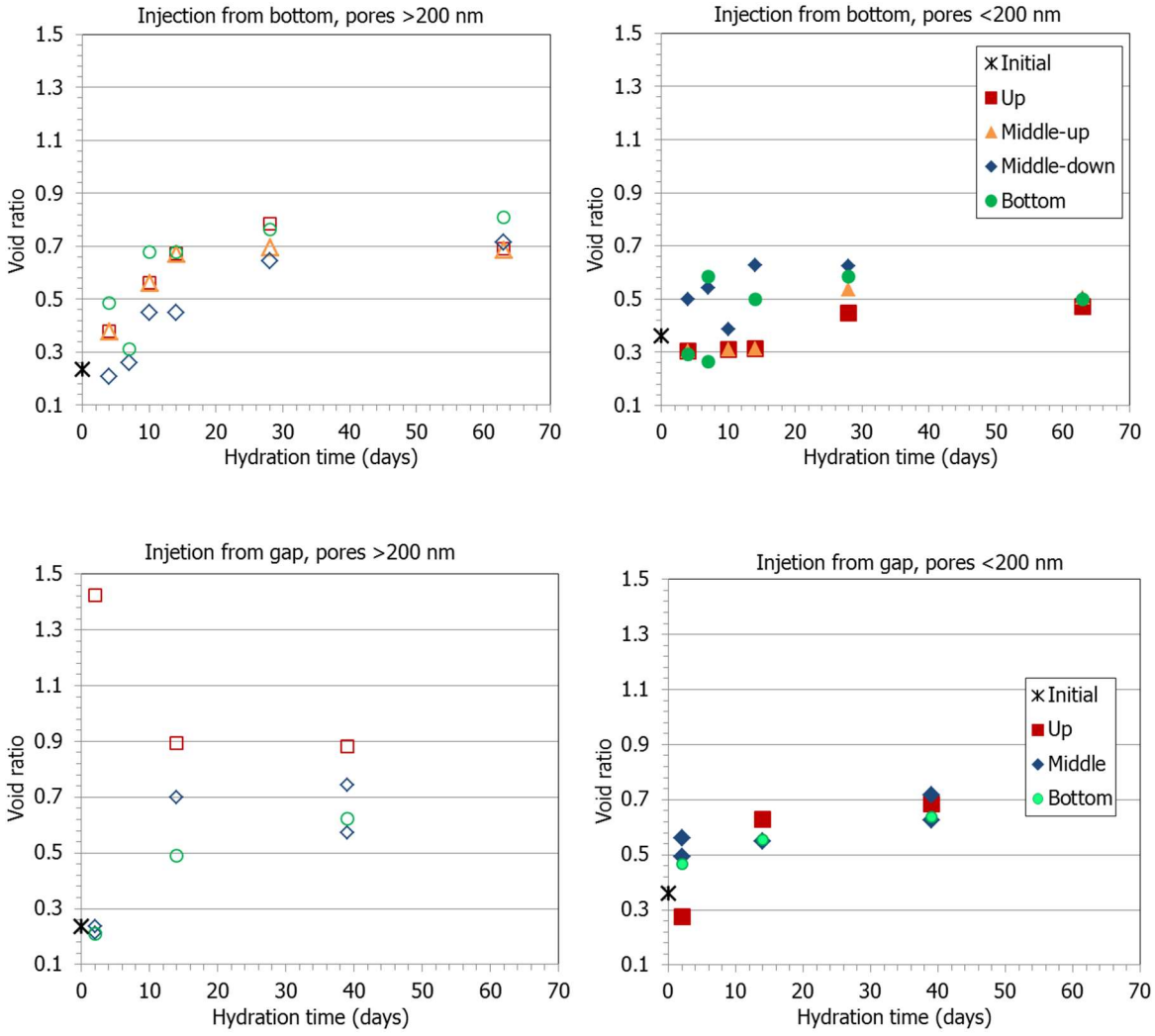

Figure 12. Evolution of void ratio over time corresponding to pores larger and smaller than 200 nm for subsamples of the two sets of GAP-liquid tests taken at different heights along the bentonite blocks. The crosses indicate the values for the initial sample (time 0)

As a result of these changes, the ratio between the void ratios corresponding to pores smaller (e_m) and larger (e_M) than 200 nm significantly decreased for the longer tests (Fig. SM10). In the case of the samples saturated through the gap this ratio was lower for the subsamples closer to the gap, where the bentonite could freely and quickly swell. It is remarkable that, in the tests with hydration through the bottom, this ratio was the same across the sample after 28 and 63 days, and in the samples saturated through the gap it was the same after 14 and 39 days, further confirming the "steady conditions" mentioned above, which were also shown by the water content and dry density distributions (Figure 10).

5 Discussion

The evaluation of the results obtained in the two kinds of cells indicates that the hydration kinetics was affected by the actual suction and by the position of the gap with respect to the hydration source. The final water content of the samples saturated via vapour transfer was related to the water retention curve, with an equilibrium value in the case of the tests under suction 0.5 MPa slightly above that expected for bentonite of similar dry density (1.44 g/cm^3) subjected to the same suction under confined conditions (Figure 13). This could imply that the application of a low suction under constrained conditions or under permitted swelling (although limited) affected the final equilibrium water content, which would be lower in the first case (constant volume) even if the final dry density of the bentonite was the same. In any case, the final swelling of the samples under suction 6 MPa was not enough as to close the gap, which would have meant a 20% swelling. The samples saturated under the lowest suction (0.5 MPa) were able to swell enough as to close the gap before the equilibrium water content had been reached. These samples could have taken more water if swelling had been allowed and their dry density had reached a lower value. Indeed under a given vertical stress (null in the case of the GAP tests) the swelling capacity increases with the decrease in suction (e.g. [31], [32], [33], [34], [35]). In fact, samples of FEBEX bentonite of initial dry density 1.70 g/cm^3 submitted in an oedometer to suction 4 MPa under a vertical stress of 0.1 MPa recorded an axial swelling of 17% after 118 days (sample diameter 3.8 cm, as in the GAP-vapour tests) and of 21% after 524 days (sample diameter 5 cm), whereas the latter sample submitted to a suction of 1 MPa recorded an axial swelling of 29% [36]. Although the conditions were not exactly the same (in the oedometer a small axial load was applied to the samples, and the different diameter may affect the friction role), these values seem consistent with the strains observed in the GAP-vapour tests.

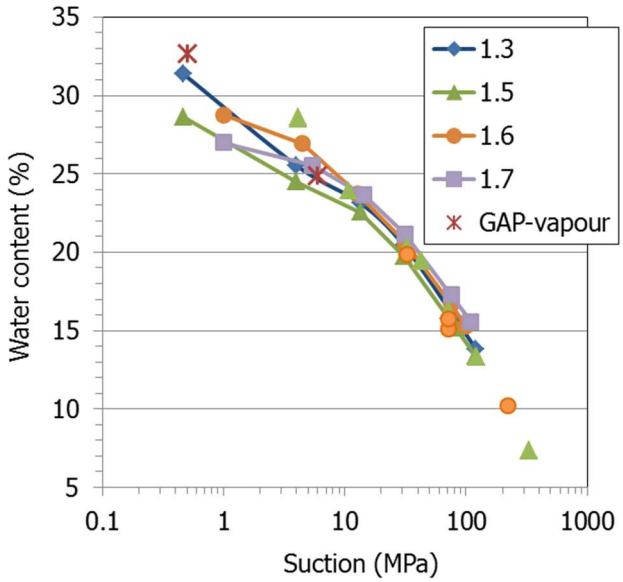

Figure 13. Equilibrium values reached in the GAP-vapour tests (average of 6 tests for each suction) and water retention curves of FEBEX bentonite compacted to different dry densities (indicated in g/cm³) obtained under isochoric conditions (results from Villar 2007, Villar et al. 2012 and unpublished)

In the GAP-vapour tests the final overall water contents were lower and the dry densities higher than in the GAP-liquid tests, because the void height was larger in the latter (9 mm vs. 5 mm, corresponding to a potential swelling of 32 vs. 20%). As a result of the higher dry density of the GAP-vapour tests, and despite their lower water content, the final degree of saturation of the tests performed under suction 0.5 MPa was in the order of the GAP-liquid tests (Figure 14). It is remarkable that, in the first stages of hydration (times less than 10 days) of the GAP-liquid tests hydrated from gap, the degree of saturation of the samples decreased below the initial one, which was due to the significant decrease of dry density allowed by the almost "free" swelling into the gap.

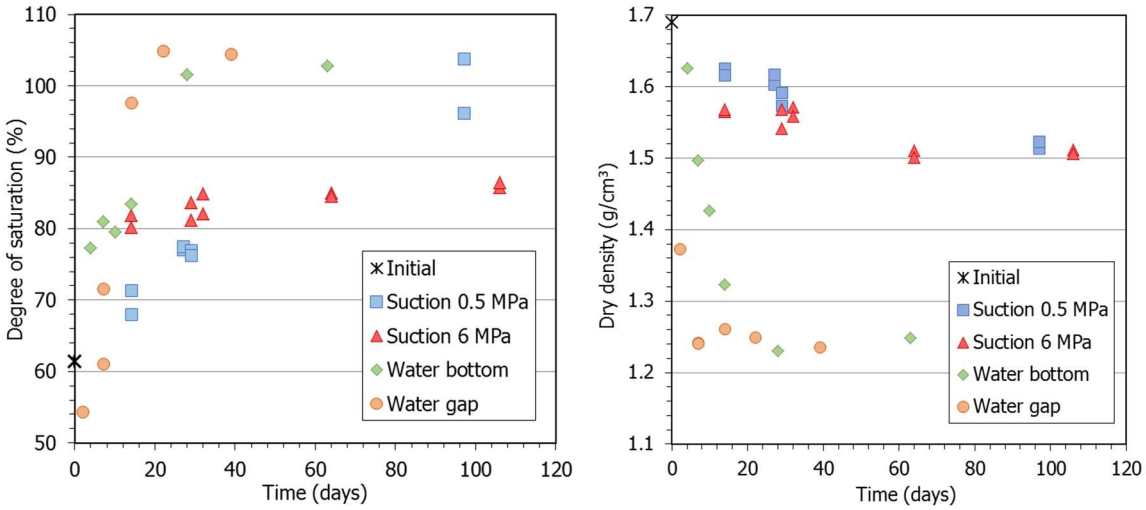

Figure 14. Evolution of the degree of saturation and dry density in tests of all kinds shorter than 100 days

Although the flow rate prescribed in the two kinds of tests performed with liquid water was the same, when water was supplied through the gap, the samples were able to swell into the open void and take water immediately (because of the higher permeability of the swollen, low-density bentonite, in which also the void ratio corresponding to macropores allowing water flow was very high), developing higher internal dry density and water content gradients (Figure 10). In the tests with hydration from the opposite side to the gap, no free swelling was readily allowed and the permeability of the bentonite was lower because its dry density was higher (see relation between dry density and hydraulic conductivity in Equations 2 and 3) and because the void ratio corresponding to macropores was lower (Figure 12). Consequently the overall block dry density also decreased initially faster and reached earlier the lowest possible value when the bentonite was hydrated from the gap, which closed sooner. In a series of tests reported by Harrington et al. [18] in which compacted bentonite was allowed to swell into an axial void initially filled with water, the bulk of the sample expansion occurred through unconstrained swelling through the upper face of the clay (where the void was), which accounted for around 77% of the swelling strains required to close the void, even though water was also injected from the opposite surface. In fact some swelling took also place from the bottom of the sample, opposite to the gap, where water was also injected, and this would be the case of the tests reported here with injection through the bottom. In the tests by Harrington et al. [18], the swelling from the bottom roughly corresponded to 25% of the total swelling necessary to close the void (depending on the void length), which is consistent with the slower closing of the gap in the tests saturated from the bottom presented here. For similar test durations the dry density close to the hydration surface of the tests saturated through the bottom was higher than that of the

586 tests saturated through the gap (Figure 10), which would explain that water pressure developed
587 earlier in the former (Fig. SM8).

588 In turn, the irreversibility of the initial strains was related to their magnitude. Hence the gradients
589 were more remarkable and persistent when hydration took place in the water phase, then under
590 "high" suction and finally under low suction. In tests sufficiently long steady gradients were reached,
591 with no further changes in water content or dry density. Figure 15 illustrates these observations by
592 comparing the results in terms of water content and dry density for tests of different kinds long
593 enough as to have reached steady conditions. Indeed the time needed to reach "steady conditions"
594 was much longer in the GAP-vapour tests. Note that the minimum possible overall dry density and
595 maximum water content of the GAP-vapour tests were ~1.42 g/cm^3 and ~35%, and for the GAP-
596 liquid tests ~1.25 g/cm^3 and ~44%, because of the different gap dimensions. Nevertheless, no
597 completely homogeneous density or water content distribution was observed in any of the tests, and
598 the bentonite that was closer to the gap had final higher water content and lower dry density. This
599 was also observed in similar tests with axial gaps performed by Watanabe and Yokoyama [37] in
600 bentonite/sand mixtures and by Dueck et al. [16], Harrington et al. [18] and Daniels et al. [38] in
601 bentonite, even though the axial and radial pressures measured had attained equilibrium.

602 The relation between way of hydration and irreversibility of strains was also put forward in tests
603 performed in binary samples, constituted by a high-density bentonite block and a lower-density
604 bentonite pellets mixture saturated either through the block or the pellets using constant water
605 injection pressure or constant flow rate, the irreversibility being more notable in the first case, where
606 saturation was quicker [19].

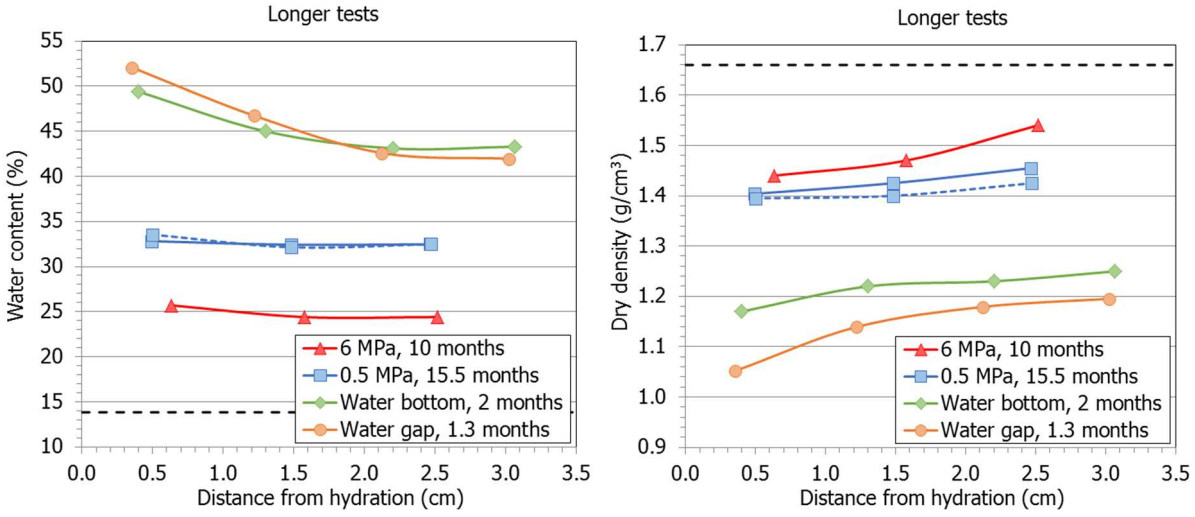

Figure 15. Final water content and dry density of subsamples of all tests long enough as to have reached steady conditions. Hydration from gap in all cases except in the "Water bottom" series. The thick discontinuous horizontal lines indicate the values for the initial sample

As discussed by Romero and Simms [26], the pore size distribution obtained by MIP is not necessarily the true distribution of pores, due to various issues including pore accessibility and sample treatment, yet it gives a useful quantitative characterization of microstructure. Because of the swelling into the gap, hydration brought about an overall increase in the void ratio corresponding to all pore sizes. However, it is remarkable that, despite the significant changes in pore size distribution occurred as a result of hydration and expansion, the limit between the two major pore families observed by MIP kept in all cases around 200 nm. This could be linked to the relatively large particle size of the untreated FEBEX bentonite (with a 50% of particles larger than 1 mm and 25% between 2 and 5 mm, see Fig. SM1) and would explain the different limit between pore families set for other materials analysed in this context in which all the particles had a size lower than 2 mm (e.g. [6], [15], [39]). Although the volume of pores smaller than 200 nm in the FEBEX bentonite was initially predominant, over time the volume of macropores increased more than that of smaller pores (Figure 7, Figure 12), giving place to an overall decrease of the ratio between the void ratio corresponding to pores smaller (e_m) and larger (e_M) than 200 nm, which also tended to be constant along the sample in the longer tests (Figure 16).

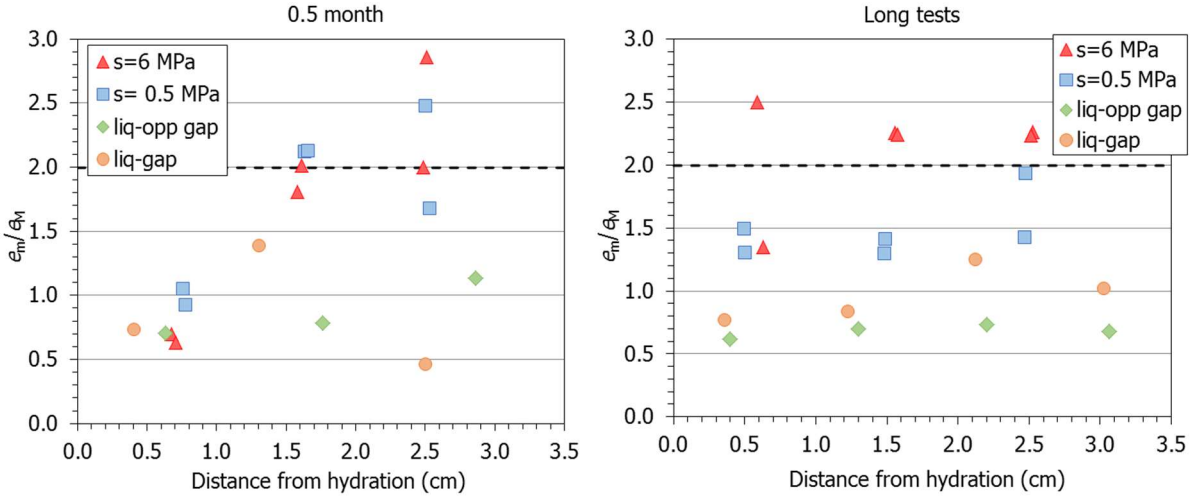

Figure 16. Ratio between void ratio corresponding to pores smaller and larger than 200 nm in tests of duration 0.5 month (left) and tests having reached steady conditions (right, same tests as in Figure 15). The thick discontinuous horizontal lines indicate the values for the initial sample

The increases in macropore void ratio took place very quickly and were much more notable in the samples saturated with liquid water, particularly in the subsamples closest to the gap (Fig. SM11), which can be related to the lower dry densities that they reached. Besides, in the samples saturated with liquid water through the gap the increase of void ratio affected all pore sizes, whereas in the samples saturated opposite to the gap it was the macropores that experienced the largest increase in void ratio, resulting in final lower e_m/e_M ratios. In the samples tested under suction, the macropore void ratio increase was also quick close to the gap, but took longer in positions away from it. The size of the macropores increased as well, but in the GAP-vapour tests the increase was more notable in the shorter ones and later the size of macropores decreased to values which were still higher than the initial one, the same trends being observed all along the samples. In contrast, the macropore size in the GAP-liquid tests increased more away from the hydration surface. The changes in void ratio corresponding to pores smaller than 200 nm were overall more uniform across the samples, although in the samples saturated with liquid water e_m increased more close to the gap. In a series of infiltration tests carried out in compacted MX80 bentonite/COx claystone mixtures with different technological voids, Zeng et al. [39] observed significant increases in large-pore and medium-pore void ratios in the areas where the swelling mixture initially filled the gaps. The increases in macropore void ratio and size observed in the samples closest to the gap, particularly at shorter times, are likely related to the cracks observed on top of some samples (Figure 5, Figure 8, Fig. SM9). Wang et al. [40] observed that the sealing of a technological void started by the formation of tensile cracks that were closed with the sealing of the void, consistently with these observations.

As a result of these changes, the e_m/e_M ratio was lower in the subsamples closest to the gap in the shorter tests, but in longer tests tended to be the same along the whole bentonite block, and lower than the initial one, which would be an additional indication of equilibrium being reached (Figure 16). Only in the tests performed under suction 6 MPa, in which the gap was not closed because of the lower equilibrium water content, the final e_m/e_M ratio was higher than the initial one.

Hydration of bentonite samples under confined conditions has been usually reported to result in an increase of micropore void ratio and a homogenization of the pore sizes towards smaller values (e.g. [41]). This was the case of the bentonite samples retrieved from the FEBEX in situ test after 18 years of operation [21] and also of binary samples of blocks and pellets saturated in an oedometer [19]. Massat et al. [42] followed with X-ray tomography the bentonite porosity evolution during swelling pressure tests and observed the progressive decrease of inter-aggregate pores as a result of saturation. In all these cases the bentonite was saturated under constant volume conditions. These observations are in contrast with the results reported here, where a general increase of the macropore void ratio and of the macropore mode size was observed, which may indicate that the presence of a gap where the bentonite swelled into really affected the kind of microstructural changes. In the FEBEX in situ test there were initially gaps close to the rock surface, but either the modifications close to the gap were too local to be observed in the general sampling performed or they had obliterated with time.

The size of the gaps considered in this research represented percentages of between 17 and 27% of the total sample volume, which are higher than what would be expected in a repository (6-14% according to the literature). Hence, although maybe in a worst-case scenario, the tests are representative of the areas closest to the voids in a real repository, where not the bulk of the barrier would be affected by the filling of the technological voids, but mainly the areas closest to them.

Overall, the results reported in this paper are consistent with the key features of behaviour underlying the homogenization processes, which according to the modelling work performed in the framework of the BEACON project would be stress path dependency and strain irreversibility [14].

6 Conclusions

In the context of the deep geological disposal of nuclear waste and to improve the understanding of the homogenization process of bentonite barriers, in particular with regards to the filling of technological voids, a series of tests were performed in compacted FEBEX bentonite cylindrical

samples hydrated under limited axial swelling conditions, i.e. with a gap on top. These samples were hydrated with water in vapour (GAP-vapour) or liquid phase (GAP-liquid) and were dismantled after different periods of time. The water content, dry density and pore size distribution at different levels along the samples were determined at the end of the tests. In the GAP-vapour tests the samples were saturated from the top surface using the vapour transfer technique, applying suctions of 6 and 0.5 MPa. In the GAP-liquid tests the bentonite was saturated with deionised water injected at a rate of 0.07 cm^3/h, either from the bottom surface or from the gap. The GAP-vapour tests would simulate a repository with limited water availability and the GAP-liquid ones a repository in a host rock with plenty of free water. From the observations and analysis reported, the following conclusions can be drawn:

- The final water content of the samples saturated via vapour transfer was approximately related to the water retention curve of the reference FEBEX bentonite obtained in isochoric tests. Since the final swelling strain is related to the final water content, if the latter is too low, swelling might not be enough as to close the gap, as it happened in the tests under suction 6 MPa. Hence, in a real repository case, if there is scarce water and the relative humidity is low (suction is high), technological voids might not be filled, because the water taken by the bentonite would be insufficient to result in enough swelling. This aspect had not been put forward in previous related investigations in which plenty of liquid water was used to hydrate the bentonite.
- The hydration kinetics (considered as the pace of increase in overall water content) was affected by the actual suction, being slower under the lowest suction. In turn, the strain development was also affected by the spatial configuration. When liquid water was supplied through the gap, the samples were able to swell into the open void, where the bentonite density was initially very low and its permeability higher, which was also confirmed by the larger macropore void ratio and size in this area. As the water content increased, the overall dry density decreased and the size of the gap reduced. Consequently the gap closed faster when hydration took place from it.
- At the end of the tests the bentonite water content was higher close to the hydration surface and its dry density lower. The faster the water content increase the larger the strains initially occurred and their irreversibility. Large initial strains resulted in steeper and more persistent gradients. Consistently with the findings of other authors, in tests sufficiently long no further changes in water content or dry density were observed, even though no completely homogeneous density or water content spatial distribution was reached.
- Because of the swelling into the gap the samples experienced an overall increase in the void ratio corresponding to all pore sizes, but the microstructural changes were quicker and more drastic

when the water content increase was faster. Although the volume of pores smaller than 200 nm (void ratio e_m) was initially higher, over time the volume of macropores (void ratio e_M) increased more than that of smaller pores, and faster closer to the gap and in the samples saturated with liquid water, giving place to an overall decrease of the e_m/e_M ratio, which also tended to be constant along the sample in the longer tests. Only in the tests performed under suction 6 MPa, in which the gap was not closed because of the lower equilibrium water content, the final e_m/e_M ratio was higher than the initial one. The size of the macropores significantly increased in the first stages, but tended to decrease over time, likely in connection with the closing of the gap. Moreover, in the first stages of hydration and in the areas closest to the gap, the volume of pores larger than the detection limit of the mercury intrusion porosimetry (550 μm) was found to be relevant and possibly resulted in an increase of the initial permeability of the samples.

The patterns described in the two last bullets cannot be extrapolated to the bulk of the barrier, since they have been obtained in tests representing the areas closest to the technological voids. With a view on future research, it must be highlighted that all the tests were performed with the same initial dry density, and that since the initial swelling seems to considerably affect the "long-term" evolution, samples with different initial dry density –or of different bentonites–, and consequently, swelling potential, may behave differently. Also the size of the gap, and consequently the minimum density that the samples may reach, is a factor that could affect the irreversibility of the strains and gradients observed. This might have played a role in the differences observed between the GAP-liquid and the GAP-vapour tests. For the samples saturated in the water phase, the effect of water injection pressure or flow rate should also be checked.

Acknowledgements

The research leading to these results was financed by the Beacon project, which receives funding from the Euratom Research and Training Programme 2014–2018 under grant agreement number 745942. Part of the laboratory work was carried out by J. Aroz. The mercury intrusion porosimetry tests were performed at the Petrophysical Laboratory of CIEMAT by N. Brea.

Data availability statement

The datasets generated during and/or analysed during the current study are available from the corresponding author on reasonable request.

CRediT statements

M.V. Villar: conceptualization, formal analysis, investigation, writing, editing, supervision

C. Gutiérrez-Álvarez: investigation, formal analysis, resources, visualization, review

G. Campos: investigation, formal analysis, resources, visualization

7 References

1. Towler, B.F. and G.C. Ehlers. *Friction Factors for Hydrated Bentonite Plugs*. in *SPE Rocky Mountain Regional Meeting*. 1997. Casper, Wyoming.
2. Towler, B.F., et al. *Field Trials of Plugging Oil and Gas Wells with Hydrated Bentonite*. in *SPE Asia Pacific Oil & Gas Conference and Exhibition*. 2016. Perth, Australia.
3. Englehardt, J., M.J. Wilson, and F. Woody, *New Abandonment Technology New Material and Placement Techniques*, in *SPE/EPA/DOE Exploration and Production Environmental Conference*. 2001: San Antonio, Texas. p. SPE 66496.
4. Clark, J. and B. Salsbury. *Well Abandonment Using Highly Compressed Sodium Bentonite - An Australian Case Study*. in *SPE/EPA/DOE Exploration and Production Environmental Conference*. 2003. San Antonio, Texas.
5. Mokni, N., et al., *Effect of technological macro voids on the performance of compacted bentonite/sand seals for deep geological repositories.* International Journal of Rock Mechanics and Mining Sciences, 2016. **88**: p. 87-97.
6. Wang, Q., et al., *The effects of technological voids on the hydro-mechanical behaviour of compacted bentonite–sand mixture.* Soils and Foundations, 2013. **53**(2): p. 232-245.
7. Villar, M.V., et al., *Physical evolution of a bentonite buffer during 18 years of heating and hydration.* Engineering Geology, 2020. **264**: p. 105408.
8. García-Siñeriz, J.L., et al., *Engineered barrier of bentonite pellets and compacted blocks: State after reaching saturation.* Engineering Geology, 2015. **192**(0): p. 33-45.
9. Delahaye, C. and E.E. Alonso, *Soil Heterogeneity And Preferential Paths For Gas Migration.* Eng. Geol. 64: 251-271, 2002.
10. De la Vaissiere, R., *Hydration versus gas percolation in bentonite. In-situ experiment PGZ2. Experimental borehole results*. 2013. p. 99.
11. S., L., et al., *Initial State of the Art on Gas Transport in Clayey Materials*, in *Deliverable D6.1 of the HORIZON 2020 project EURAD, Work Package Gas. EC Grant agreement no: 847593*. 2021. p. 364.
12. Bernachy-Barbe, F., et al., *Observed heterogeneities after hydration of MX-80 bentonite under pellet/powder form.* Applied Clay Science, 2020. **189**: p. 105542.

13. Bernachy-Barbe, F., *Homogenization of bentonite upon saturation: Density and pressure fields.* Applied Clay Science, 2021. **209**: p. 106122.

14. Gens, A., *Description of the constitutive models developed in the project. Conceptual bases, mathematical description and model capabilities. Assessment of predictive power*. 2021. p. 338.

15. Bian, X., Y.-J. Cui, and X.-Z. Li, *Voids effect on the swelling behaviour of compacted bentonite.* Géotechnique, 2019. **69**(7): p. 593-605.

16. Dueck, A., et al., *Bentonite homogenisation. Laboratory study, model development and modelling of homogenisation processes*, in *Technical Reports*, S.K. AB, Editor. 2019: Stockholm. p. 78.

17. Talandier, J.E., *Synthesis of results from task 5.1. BEACON Deliverable D5.1.2.* . 2019. p. 334.

18. Harrington, J.F., et al., *Bentonite homogenisation during the closure of void spaces.* International Journal of Rock Mechanics and Mining Sciences, 2020. **136**: p. 104535.

19. Villar, M.V., et al., *Pellets/block bentonite barriers: Laboratory study of their evolution upon hydration.* Engineering Geology, 2021. **292**: p. 106272.

20. ENRESA, *FEBEX Full-scale Engineered Barriers Experiment, Updated Final Report 1994-2004*. Publicación Técnica ENRESA Vol. 05-0/2006. 2006, Madrid: ENRESA. 590.

21. Villar, M.V.E., *FEBEX-DP Postmortem THM/THC Analysis Report*, in *NAGRA Arbeits Bericht*, NAGRA, Editor. 2017. p. 143.

22. Villar, M.V., *Thermo-hydro-mechanical characterisation of a bentonite from Cabo de Gata*. Publicación Técnica ENRESA. Vol. 04/2002. 2002: ENRESA.

23. Villar, M.V., *Water retention of two natural compacted bentonites.* Clays and Clay Minerals, 2007. **55**(3): p. 311-322.

24. Villar, M.V., R. Gómez-Espina, and L. Gutiérrez-Nebot, *Basal spacings of smectite in compacted bentonite.* Applied Clay Science, 2012. **65-66**: p. 95-105.

25. Villar, M.V., et al., *Effect of prolonged drying at high temperature on the water retention capacity of bentonite (FEBEX-DP samples).* Applied Clay Science, 2019. **182**: p. 105290.

26. Romero, E. and P.H. Simms, *Microstructure Investigation in Unsaturated Soils: A Review with Special Attention to Contribution of Mercury Intrusion Porosimetry and Environmental Scanning Electron Microscopy.* Geotechnical and Geological Engineering, 2008. **26**(6): p. 705-727.

27. Yuan, S., X. Liu, and O. Buzzi, *Technical aspects of mercury intrusion porosimetry for clays.* Environmental Geotechnics, 2021. **8**(4): p. 255-263.

28. Sánchez, M., et al., *A double structure generalized plasticity model for expansive materials.* International Journal for Numerical and Analytical Methods in Geomechanics, 2005. **29**(8): p. 751-787.

29. Yuan, S., et al., *Discussion on the separation of macropores and micropores in a compacted expansive clay.* Géotechnique Letters, 2020. **10**(3): p. 454-460.

30. Sing, K.S.W., et al., *Reporting Physisorption Data For Gas/Solid Systems.* Pure And Appl. Chem. 57(4): 603-619, 1985.

31. Lloret, A., et al., *Mechanical behaviour of heavily compacted bentonite under high suction changes.* Géotechnique, 2003. **53**(1): p. 27-40.

32. Delage, P., M.D. Howat, and Y.J. Cui, *The Relationship Between Suction And Swelling Properties In A Heavily Compacted Unsaturated.* Engineering Geology, 1998. **50**: p. 31-48.

33. Cuisinier, O. and F. Masrouri, *Hydromechanical behaviour of a compacted swelling soil over a wide suction range.* Engineering Geology, 2005. **81**(3): p. 204-212.

34. Yigzaw, Z.G., et al., *Role of different suction components on swelling behavior of compacted bentonites.* Applied Clay Science, 2016. **120**: p. 81-90.

35. Zhang, Z., et al., *Mechanical behavior of GMZ bentonite pellet mixtures over a wide suction range.* Engineering Geology, 2020. **264**: p. 105383.

36. Villar, M.V. and A. Lloret, *Bentonite strain due to cyclic suction changes*, in *Unsaturated soils. The 7th International Conference on Unsaturated Soils 2018 (UNSAT2018)*, C.W.W. Ng, et al., Editors. 2018, Hong Kong University of Science and Technology: Hong Kong. p. 557-562.

37. Watanabe, Y. and S. Yokoyama, *Self-sealing behavior of compacted bentonite–sand mixtures containing technological voids.* Geomechanics for Energy and the Environment, 2021. **25**: p. 100213.

38. Daniels, K.A., et al., *Closing repository void spaces using bentonite: does heat make a difference?* Applied Clay Science, 2021. **210**: p. 106124.

39. Zeng, Z., et al., *Effects of technological voids and hydration time on the hydro-mechanical behaviour of compacted bentonite/claystone mixture.* Géotechnique, 2022. **72**(1): p. 34-47.

40. Wang, Q., et al., *Cracking and sealing behavior of the compacted bentonite upon technological voids filling.* Engineering Geology, 2021. **292**: p. 106244.

41. Schanz, T. and Y. Al-Badran, *Swelling pressure characteristics of compacted Chinese Gaomiaozi bentonite GMZ01.* Soils and Foundations, 2014. **54**(4): p. 748-759.

42. Massat, L., et al., *Swelling pressure development and inter-aggregate porosity evolution upon hydration of a compacted swelling clay.* Applied Clay Science, 2016. **124–125**: p. 197-210.